Powder Technology 331 (2018) 244–249

Contents lists available at ScienceDirect

Powder Technology

journal homepage: www.elsevier.com/locate/powtec

A novel green-emitting phosphor of Ce^{3+}-activated $CaGd_4F_{14}$: Synthesis, high efficiency, and thermal stability

Zhiwen Gao [a], Lei Zhao [b], Jianyue He [a], Ruijin Yu [a,*]

[a] College of Chemistry & Pharmacy, Northwest A&F University, Yangling, Shaanxi 712100, PR China
[b] Institute of Physics and Optoelectronics Technology, Baoji University of Arts and Sciences, Baoji 721016, PR China

ARTICLE INFO

Article history:
Received 10 August 2017
Received in revised form 4 March 2018
Accepted 7 March 2018
Available online 15 March 2018

Keywords:
Phosphor
Fluoride
Photoluminescence
Ce^{3+}
Thermal stability

ABSTRACT

A new green-emitting phosphor of Ce^{3+}-doped $CaGd_4F_{14}$ (1–15 mol%) was synthesized by a facile solid-phase reaction. The crystal phase was investigated via X-ray polycrystalline powder diffraction (XRD) and Rietveld refinement. The scanning electron microscopy (SEM), photoluminescence (PL), decay lifetime and quantum efficiency (QE) were applied to characterize the phosphor. The phosphor shows the excitable wavelength in the UV region of (220–320 nm). $CaGd_4F_{14}$:Ce^{3+} has a green-emission band from 400 to 625 nm with maximum wavelength at 525 nm, which is the typical electronic transitions of 4f-5d of Ce^{3+}-ions. The maximum QE was measured to be 67%. And the phosphor presents good thermal luminescence stability on temperature quenching. The thermal quenching energy is 0.503 eV. This phosphor has a potential application in lighting and display.

1. Introduction

In the past decades, Rare-earth ions (RE)-activated fluorides have been intensively reported because of the potential applications in excellent luminescence, displays devices, optical amplifiers and biological labels [1–5]. Compared with RE-doped oxides, fluoride phosphors have excellent thermal stabilities due to their low energy phonons and therefore the quenching of excited states of the RE ions are minimal [6–8]. For example, Ce^{3+} ion is one of the most important RE activators in fluoride phosphors.

The 4f state of Ce^{3+} ion only has one electron, and two ground states of $^2F_{7/2}$ and $^2F_{5/2}$ have a difference of about 2200 cm^{-1} due to spin–orbit coupling [9]. Generally, the local crystal fields play an important role on the emission of Ce^{3+} ion [10,11]. It has been widely reported that Ce^{3+} ion-activated fluorides could present typical broad UV emission with high luminescence quantum efficiencies at indoor temperature. In these years, a great number of references about the luminescent properties of RE-activated fluorides and oxyfluorides have been reported [12–15].

Gd-containing fluorides are excellent hosts as RE-activated phosphors. On account of the ^8S–^6P transitions of Gd^{3+} ion could overlap with the 4f–5d absorption bands of Ce^{3+}, Gd^{3+} ion as an intermediate can facilitate the excited energy to migrate over Gd^{3+} sub-lattice in Gd-fluorides [16]. This is favorable for the improvement of luminescence efficiencies in Ce^{3+}-doped Gd-based compounds. This effect has been well confirmed in Ce^{3+}-doped Gd-containing fluorides [17].

In this work, Ce^{3+} ion was selected as an activator in $CaGd_4F_{14}$. The phosphors were prepared by the facile solid-state synthesis. The structure was investigated by powder X-ray powder diffraction (XRD) and refinements. The efficient green emission, high QE, and thermal activation energy (ΔE) were reported.

2. Experimental

Ce^{3+} (1–15 mol%)-doped $CaGd_4F_{14}$ polycrystalline phosphors were synthesized via solid-state reaction in two-step processing. The stoichiometric reactants of CaF_2, GdF_3 and CeF_3 (99.99%) were decided on the formula of $CaGd_4F_{14}$:$x$$Ce^{3+}$ ($x = 0.01$–0.15). Firstly, the mixed raw materials were pressed into pellets, which were then slowly heated up to 850°C for 4 h in corundum crucibles in reducing atmosphere. Secondly, the samples were finely ground and then pressed the powders into pellets again, which were heated up to 1000°C for 6 h in reducing atmosphere of 5:95 (H_2/N_2).

XRD pattern was measured via a Rigaku D/Max diffractometer equipped with Bragg-Brentano geometry. The Cu-Kα radiation ($\lambda = 1.5405$ Å) was applied with operating conditions of 40 kV, 30 mA. Rietveld structural refinement was finished using the GSAS (general structure analysis system) program. PL results were tested

---

* Corresponding author.
E-mail address: yuruijin@nwsuaf.edu.cn (R. Yu).

https://doi.org/10.1016/j.powtec.2018.03.013
0032-5910/

via Perkin-Elmer LS-50B spectrometer equipped by monochrometers (Monk–Gillieson).

A 266 nm pulsed Nd:YAG laser was applied as an excitation to measure the decay curves. The signals were collected via 75 cm monochromator with PMT (Hamamatsu R928). A digital storage oscilloscope (LeCloy 9301) was used to record the data. The data was displayed and recorded with the LeCloy 9301 digital storage oscilloscope.

3. Results

3.1. Phase formation and structure

The phase formation of the samples was checked by powder XRD measurement. No impurity lines were observed on the XRD patterns indicating the single phase of the phosphor. The representative XRD structural refinements of $CaGd_4F_{14}$:Ce^{3+} phosphors were carried out using GSAS (general structure analysis system) program. Fig. 1 displays the typical results from the refinements of $CaGd_4F_{14}$:0.1Ce^{3+}. The refined parameters and atom positions are listed in Tables 1 and 2, respectively. The results indicated that $CaGd_4F_{14}$:$x$$Ce^{3+}$ phosphors with the single phase were obtained. And the $CaGd_4F_{14}$ host can well accommodate the RE ions in the lattices.

The sketch map of $CaGd_4F_{14}$ (Fig. 2a) was modeled by using the refined atom positions. The fluoride possesses trigonal structure, which can be described with the space group $P\overline{3}c_1$ (165). The structure contains one type of 4f cations randomly occupied by Ca^{2+} and Gd^{3+} ions (Fig. 2b). The edge-shared MF_9 (M = Ca, Gd) polyhedral form the framework. Ionic radius of Ce^{3+} (1.196 Å, CN = 9) is close to Ca^{2+} (1.18 Å, CN = 9) and Gd^{3+} (1.07 Å, CN = 9) ions. It is reasonable that Ce^{3+} could replace both Ca^{2+} and Gd^{3+} sites in the lattice.

To confirm the crystalline morphology, SEM image was investigated. The scanning electron microscope photograph of Ce^{3+}-doped $CaGd_4F_{14}$ phosphors sintered at 1000 °C is shown in Fig. 3(a). The sample consists of uniform particles with the average size of 1.7 μm (Fig. 3(b). The components of as-prepared $CaGd_4F_{14}$ phosphors were characterized by energy-dispersive X-ray spectroscopy (EDS) analyses. The results for pure- and 5 mol% Ce^{3+}-doped $CaGd_4F_{14}$ are shown in Fig. 3(c) and (d), respectively. The results are in good agreement with the stoichiometric formula.

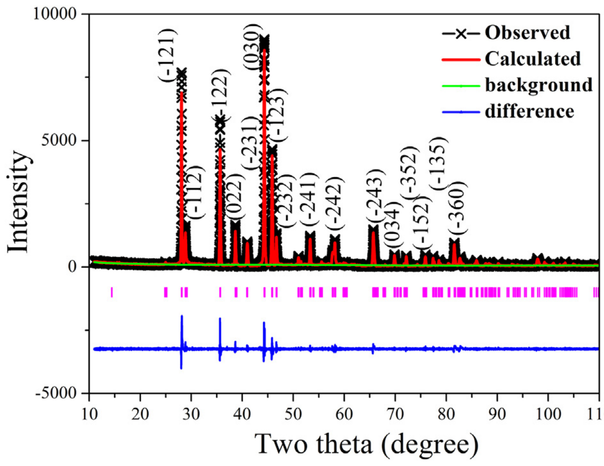

Fig. 1. The Rietveld structural refinement of $CaGd_4F_{14}$:0.1Ce^{3+}. It shows the representative experimental (crossed) and calculated (red solid line) X-ray diffraction profiles. The difference profile is located at the bottom of the figure. The main diffraction peaks were indexed.

Table 1
The refined structure unit cell parameters of $CaGd_4F_{14}$.

Formula	$CaGd_4F_{14}$
Radiation	Cu Ka
2θ range (degree)	5–110
Symmetry	Trigonal
Space group#	P-3c$_1$ (165)
a/Å	6.8681(28)
b/Å	6.8681(28)
c/Å	7.0661(4)
α/°	90
β/°	90
γ/°	120
Z	6
R_p	0.1057
R_{wp}	0.0967
X^2	7.3612
V/Å^3	288.652 (30)

3.2. The luminescence and decay lifetime

Fig. 4(a) shows the PL excitation and emission spectra of $CaGd_4F_{14}$:$x$$Ce^{3+}$. No luminescence could be detected in the pure host. Therefore, the wide bands should be from 5d–4f transitions of Ce^{3+}. Fig. 4 (a) shows an excitation band (220–320 nm) from 4f–5d transitions of Ce^{3+}. The observed sharp excitation lines from Gd^{3+} ions confirm that the energy transfer from Gd^{3+} sub-lattices to Ce^{3+} ions. The phosphors present a green-luminescence band from 400 to 625 nm with maximum wavelength at 525 nm.

Ce^{3+}-doped fluorides have been widely reported to show blue luminescence, for example, GdF_3, LaF_3, LuF_3 or CeF_3 (290–310 nm) [17], $NaGdF_4$:Ce^{3+} (360 nm) [18], $Gd_{0.5}Y_{0.5}F_3$:Ce (310 nm) [19], etc. It can be noted that $CaGd_4F_{14}$:Ce^{3+} phosphors possess a much longer emission than the reported fluorides.

In Ce-doped fluorides, it is a common fact that “perturbed Ce” centers associated with the emissions of somewhat lower energy could be easily induced due to some perturbing defects such as fluorine vacancy, or oxygen contamination [20]. It could be suggested that “Ce-perturbed” emission centers in $CaGd_4F_{14}$:Ce^{3+} can be created due to the random occupation of Ce^{3+} on Ca^{2+} and Gd^{3+} sites. Defects could be accordingly created in order to keep the charge balance. In Ce^{3+}-activated $CaGd_4F_{14}$, Ca and Gd randomly occupy the M1 site (6f) in the lattices. The occupation of Ca^{2+} positions by Ce^{3+} could result in positive charge $(Ce^{3+}{}_{Ca})^{\bullet}$. The required charge compensation can probably be achieved by possible mechanisms such as interstitial F_i' ion or cation vacancy V_{Ca}'': $[(Ce^{3+}{}_{Ca})^{\bullet} - F_i']$ or $[2(Ce^{3+}{}_{Ca})^{\bullet} - V_{Ca}'']$. The related defects could induce “Ce-perturbed” emission centers in $CaGd_4F_{14}$ lattices.

The broad emission in Fig. 4(b) was given in three Gaussian decomposition with the maximum of 18,000 cm^{-1} (Xc_1) (555 nm), 19,930 cm^{-1} (Xc_1) (501 nm), and 22,000 cm^{-1} (454 nm) via the Gaussian decomposition method. The energy difference between the sub-bands Xc_1 and Xc_2 in Fig. 4(b) is about 1930 cm^{-1}. This implies that there are at least two types of Ce^{3+} centers in the lattice [9]. However, only one crystallographic cationic site (4f) is available for Ce^{3+}

Table 2
The crystallographic positions of unit cell structure of $CaGd_4F_{14}$.

Atom	Wyck.	S.O.F.	x/a	y/b	z/c	U[Å^2]
F1	12 g	0.93	0.3561	0.3281	0.09612	0.0003
M1	6f	1	1/3	0	1/4	0.0003
F2	4d	0.93	1/3	2/3	1/6	0.0003
F3	2a	0.93	0	0	1/4	0.0003

*M1 = Ca, Gd.